END
DATE
FILMED
12 82
DTC

MICROCOPY RESOLUTION TEST CHART

NATIONAL BUREAU OF STANDARDS-1963-A

AD A121041

Cold-Air Performance of Compressor-Drive Turbine of Department of Energy Upgraded Automobile Gas Turbine Engine

II - Stage Performance

Richard J. Roelke and Jeffrey E. Haas

DTIC FILE COPY

DTIC
ELECTE
NOV 4 1982

S D

A

NASA

82 11 03 057

Cold-Air Performance of Compressor-Drive Turbine of Department of Energy Upgraded Automobile Gas Turbine Engine

II - Stage Performance

Richard J. Roelke
Lewis Research Center
Cleveland, Ohio

Jeffrey E. Haas
Propulsion Laboratory
AVRADCOM Research and Technology Laboratories
Lewis Research Center
Cleveland, Ohio

NOTICE

Summary

The aerodynamic performance of the compressor-drive turbine of the DOE Upgraded Gas Turbine (UGT) engine was determined in low-temperature air. The nominal turbine-inlet temperature was 320 K. Inlet pressures were varied between 0.4 and 2.4 bars absolute. The turbine blading used in these tests consisted of duplicates of the stator and rotor castings used in development engine tests. The as-received cast rotor blades had a significantly thicker profile than design and a fairly rough surface finish. Because of these blade profile imperfections three turbine rotor configurations were evaluated. These were the as-cast rotor, a reduced-roughness rotor, and a rotor with the blade profiles thinned to near the design profile. Tests to determine the effect of Reynolds number on the turbine performance were also made.

The turbine efficiency with the as-cast rotor at design equivalent speed and work factor was 0.783. Test results showed an increase of 1.1 points in efficiency from smoothing the surface finish and another 3.1 points from thinning the rotor profiles. The turbine performance of both the as-cast and reduced-roughness rotor configurations changed with Reynolds number. There was very little effect of Reynolds number on turbine performance with the smooth, thin rotor blades. An equation commonly used to predict the change in efficiency with Reynolds number did not satisfactorily predict the measured results. A comparison between the UGT compressor-drive turbine and the compressor-drive turbine of the DOE baseline gas turbine engine showed that the UGT turbine achieved a 2-point improvement in efficiency.

Introduction

The Department of Energy (DOE) is sponsoring an engine research program to demonstrate an automobile powered by a gas turbine engine of contemporary design with drivability characteristics and fuel economy that can compete with those of a conventionally powered automobile. In 1972 the Chrysler Corporation's sixth-generation prototype gas turbine engine was selected as the baseline engine. Under an interagency agreement the NASA Lewis Research Center obtained the turbomachinery components from the baseline engine and were given the responsibility for evaluating the aerodynamic performance of the components. The DOE contract with Chrysler was later amended to include the design, building, rig testing, and road demonstration of an Upgraded Gas Turbine (UGT) engine. This was a new engine designed for a smaller vehicle and intended to meet the Federal emission standards with a significant improvement in fuel economy over that of the baseline engine. A general description and some of the design features of the UGT engine are given in reference 1. Lewis was assigned the tasks of the aerodynamic design and testing of the compressor, the compressor-drive turbine, and the power turbine. The aerodynamic designs of these components are described in references 2 to 4.

The aerodynamic design of the compressor-drive-turbine inlet manifold and the mechanical designs of all the turbomachinery components were performed by the Chrysler Corporation. The experimental evaluation of the compressor is still under way, and the performance determination of the engine configuration of the power-turbine is presented in reference 5. The experimental evaluation of the compressor-drive turbine is covered in this report plus references 6 and 7. Reference 8 is the final contractor's report for the UGT engine program.

The experimental evaluation of the compressor-drive turbine was performed in two phases. The first phase was an evaluation of the inlet manifold and stator assembly to determine (1) the losses within the manifold, (2) the conditions of the flow entering and leaving the stator, and (3) the stator blading performance. The results are presented in reference 6.

The second phase of the program, which is the subject of this report, was an evaluation of the overall stage performance. The turbine blading used in these tests consisted of as-cast hardware representative of the stator and rotor castings used in the test and vehicle engines. Initially, aerodynamic performance of the as-cast blading was obtained over a range of turbine equivalent speed and pressure ratios. Because inspection of the rotor blading before the start of the turbine component tests showed significant deviations from design in the profile shape and a fairly rough surface, two additional turbine builds were tested in which the as-cast rotor blading was modified. One configuration had reduced rotor blade surface roughness, and the other configuration had the rotor blade profiles reworked to more nearly approach the design profile. The stator was not modified in these tests. The measured effect and an analysis of these blading modifications on the turbine performance are reported in reference 7 and summarized in this report. Finally, all three rotor configurations were tested over a range of inlet total pressures at design equivalent speed to evaluate Reynolds number effects.

The stage performance of the as-cast turbine blading was determined with air at a nominal inlet temperature of 320 K and an inlet pressure of 0.8 bar absolute. Performance data were taken at total-to-total pressure ratios from 1.3 to 2.7 and rotative speeds from 50 to 110 percent of equivalent design speed. During the performance tests with the two modified rotors, data were taken only at equivalent design speed. Rotor-exit radial surveys of total pressure, total temperature, and flow angle were made at equivalent design speed and

design work factor for all three rotor configurations. The Reynolds number tests were conducted at different values of turbine-inlet pressure. The inlet pressure was varied from 0.4 to 2.4 bars absolute, resulting in Reynolds numbers from 1.2×10^5 to 8.0×10^5.

The aerodynamic performance of the compressor-drive turbine is presented in terms of equivalent mass flow, torque, specific work, and efficiency. A comparison is made between the aerodynamic performance of the subject turbine (with the reworked rotor blades) and the compressor-drive turbine from the baseline gas turbine engine.

Symbols

A	coefficient used in eq. (1)
AR	blade aspect ratio based on actual chord length
B	coefficient used in eq. (1)
c	actual chord, cm
Δh	specific work, J/g
m	mass flow rate, kg/sec
N	rotative speed, rpm
p	absolute pressure, bars
R_x	rotor reaction, $(p_{5.5} - p_{6.3})/(p'_{4.5} - p_{6.3})$
r	radius, m
Re	turbine Reynolds number, $m/\mu r_m$
s	blade spacing, cm
T	absolute temperature, K
U	blade velocity, m/sec
V	absolute gas velocity, m/sec
ΔV_u	change in absolute tangential velocity, m/sec
W	relative gas velocity, m/sec
α	absolute gas flow angle measured from axial direction, deg
β	relative gas flow angle measured from axial direction, deg
γ	ratio of specific heats
δ	ratio of inlet total pressure to U.S. standard sea-level pressure, $p'_{4.5}/p^*$
ϵ	function of γ used in relating parameters to those using air inlet conditions at U.S. standard sea-level conditions, $(0.740/\gamma)\,[(\gamma+1)/2]^{\gamma/(\gamma-1)}$
η'	efficiency based on total pressure ratio $p'_{4.5}/p'_{6.3}$
θ_{cr}	squared ratio of critical velocity at turbine-inlet temperature to critical velocity at U.S. standard sea-level temperature, $(V_{cr}/V^*_{cr})^2$
μ	viscosity, kg/m sec
τ	torque, N-m

Subscripts:

cr	condition corresponding to Mach 1
h	hub
m	mean
meas	measured
sur	survey
t	tip
1	subscript used in eq. (1)
2	subscript used in eq. (1)
4.5	station at manifold inlet (fig. 1)
5	station at stator inlet (fig. 1)
5.5	station at stator exit (fig. 1)
6	station located about half an axial chord downstream of rotor (fig. 1)
6.3	station located about three axial chord lengths downstream of rotor (fig. 1)

Superscripts:

'	absolute total state
*	U.S. standard sea-level conditions (temperature, 288.15 K; pressure, 1.013 bars)

Turbine Design

The UGT compressor-drive turbine is a single-stage, axial-flow design having a rotor tip diameter of 11.15 cm and stator and rotor blade heights of nominally 1.12 cm. A cross section of the turbine as it appeared in the test rig is shown in figure 1. The duplicate engine parts used in the test rig are the inlet manifold, the stator ring, and the
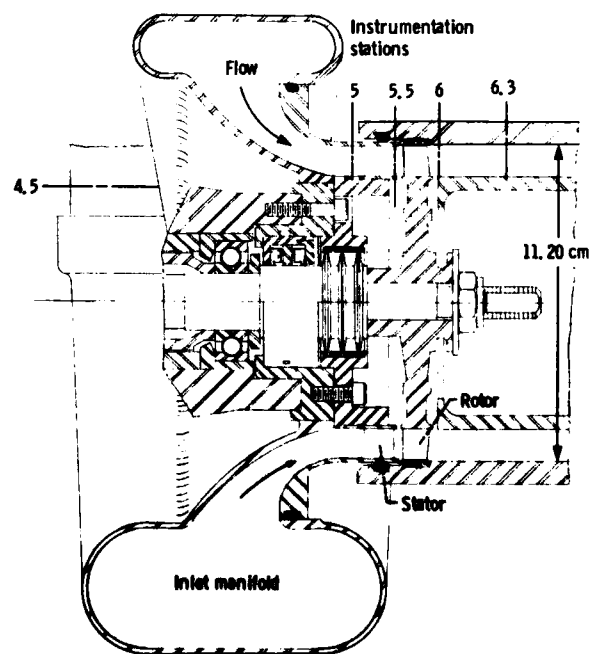

Figure 1. - Cross section of upgraded compressor-drive turbine.

2

rotor. The instrumentation stations shown in figure 1 are discussed in the section **Research Equipment and Procedure**.

The hot-engine and equivalent design conditions are listed in table I. The turbine hardware was fabricated undersized so that the flow passage would expand to the design area when the engine was operating at the design inlet temperature. Thus, it is necessary to show the equivalent flow conditions for both hot and cold hardware. The design mass flow rate is 0.598 kg/sec at the inlet temperature and pressure of 1325 K and 4.0 bars absolute. The design efficiency is 0.85 at a work factor of 2.1. The turbine design velocity diagrams are shown in figure 2. The stator-exit flow angle averages about 66.5°, and the rotor-exit relative flow angle averages about 54.5°.

The stator and rotor profiles are shown in figure 3. The inlet manifold, stator, and rotor are shown in figure 4. The manifold is volute shaped with a single entry port, and this imparts swirl to the flow. The swirling flow leaves the volute and is accelerated in an axisymmetric duct to the stator inlet. The stator has 15 blades, an aspect ratio of 0.484, and a small amount of blade camber. Table II lists design parameters for the stator.

Initially, two rotors that met the aerodynamic performance requirements were designed – one with 56 blades and the other with 62 blades. Reference 3 details the stage aerodynamic design with the 56-blade rotor. However, as discussed in reference 8, this design was not selected but was replaced with a 62-blade rotor because of high untwist blade stresses and the probability of blade

resonance in the engine operating range of the 56-blade rotor. Details of the 62-blade rotor design are presented in table III. The aspect ratio is 1.219 and the average trailing-edge blockage is about 11.8 percent. The rotor blades were designed with incidence angles ranging from $+3.1°$ to $-0.4°$ and rotor reaction R_x ranging from 0.134 to 0.347 from hub to tip, respectively. The design rotor blade surface velocities are shown in figure 5. These were obtained by using the computer program described in reference 9. Diffusion is indicated on the pressure surface of all three sections and on the suction surface at the tip section. The rotor is unshrouded and operated in the component performance tests with a tip clearance of nominally 1.7 percent of the rotor blade height.

The turbine exhaust is a constant-area duct as shown in figure 1. In the engine the compressor-drive turbine exhaust is a diffusing interstage duct, which is the inlet to the power turbine. However, for the component tests, a constant-area exhaust duct was used so that the instrumentation could be located a distance downstream where there were no rotor wake effects and where the static pressure would not be affected by the diffusion process.

Research Equipment and Procedure

The apparatus used in this investigation consisted of the research turbine, an airbrake dynamometer used to control the speed and absorb and measure the power output of the turbine, an inlet and exhaust piping system

TABLE I. - TURBINE DESIGN PARAMETERS

Parameter	Hot engine	Equivalent[a]	
		Hot hardware	Cold hardware
Turbine-inlet temperature, K	1325	288.2	288.2
Turbine-inlet pressure, bars	4.0	1.01	1.01
Mass flow rate, kg/sec	0.598	0.335	0.325
Rotative speed, rpm	58 500	27 673	27 673
Specific work, J/g	198.1	44.4	44.4
Torque, N-m	19.3	5.1	5.0
Power, kW	118.2	14.9	14.5
Turbine total pressure ratio, $P'_{4.5}/P'_{6.3}$	1.94	2.01	2.01
Total efficiency, η'	0.85	0.85	0.85
Work factor, $\Delta V_u/U_m$	2.1	2.1	2.1
Reynolds number, $m/\mu r_m$	2.44×10^5	3.74×10^5	3.69×10^5

[a]The turbine hardware was fabricated undersized so that the flow passage would expand to the design area when the turbine was operating at the hot-engine temperature. Thus the distinction between hot and cold hardware.

(a) Tip.

(b) Mean.

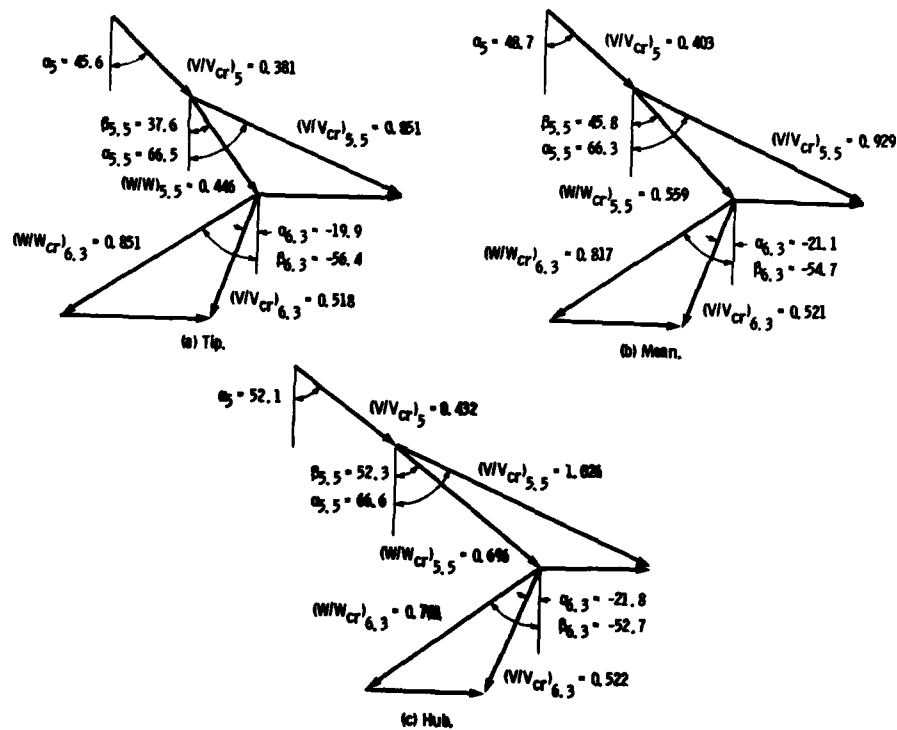(c) Hub.

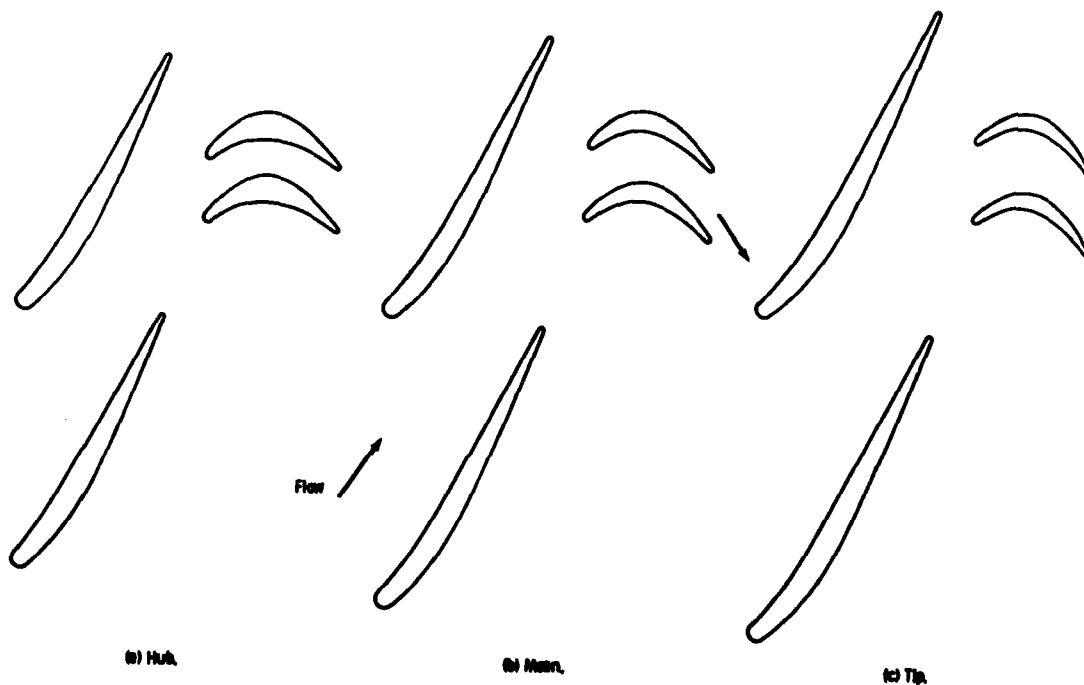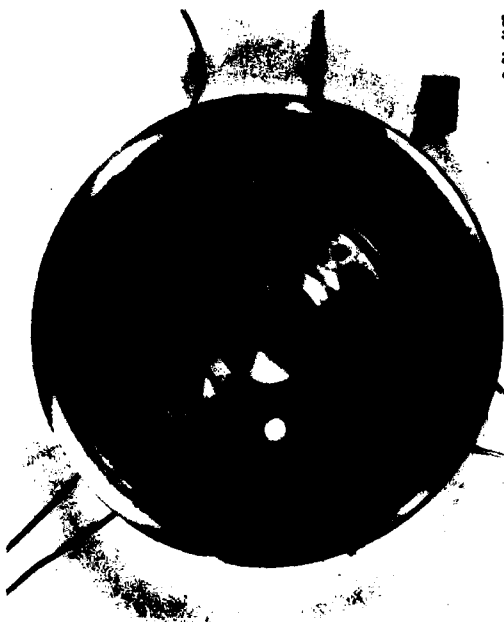Figure 2. - Design velocity diagrams.

(a) Hub.

(b) Mean.

(c) Tip.

Figure 3. - Blading profiles and flow passages.

4

(a) Inlet manifold.
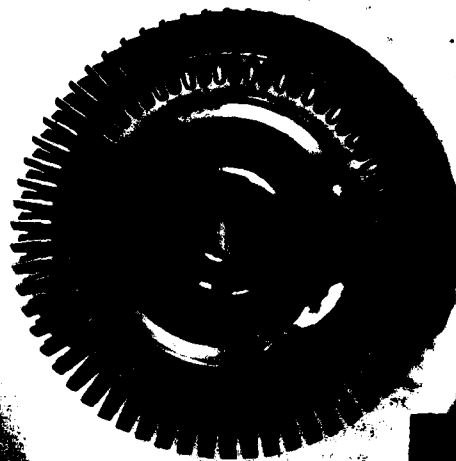
C-81-4695

(b) Stator.

C-81-4696

(c) Rotor.

Figure 4. - Compressor-drive turbine parts.

5

TABLE II. - TURBINE STATOR DESIGN PARAMETERS

Parameter	Hub	Mean	Tip
Profile radius, cm	4.445	5.004	5.563
Actual chord, cm	2.091	2.311	2.525
Axial chord, cm	1.067	1.168	1.270
Leading-edge radius, cm	0.0635	0.0635	0.0635
Trailing-edge radius, cm	0.0191	0.0191	0.0191
Trailing-edge blockage, percent	5.0	4.3	4.0
Inlet blade angle, deg	50.1	46.7	43.6
Incidence, deg	-2.0	-2.0	-2.0
Exit blade angle, deg	65.5	65.2	65.5
Solidity, c/s	1.12	1.10	1.08
Blade number	------	15	------
Blade height	------	1.118	------
Aspect ratio, AR	------	0.484	------
Radius ratio, r_h/r_t	------	0.799	------

TABLE III. - TURBINE ROTOR DESIGN PARAMETERS

Parameter	Hub	Mean	Tip
Profile radius, cm	4.445	5.010	5.575
Actual chord, cm	0.981	0.927	0.879
Axial chord, cm	0.978	0.914	0.851
Leading-edge radius, cm	0.0356	0.0330	0.0305
Trailing-edge radius, cm	0.0191	0.0191	0.0191
Trailing-edge blockage, percent	12.8	11.8	11.1
Inlet blade angle, deg	49.2	45.7	38.0
Incidence, deg	3.1	0.1	-0.4
Exit blade angle, deg	-48.3	-50.4	-52.4
Solidity, c/s	2.18	1.83	1.56
Blade number	------	62	-----
Blade height	------	1.13	------
Aspect ratio, AR	------	1.219	------
Radius ratio, r_h/r_t	------	0.797	------

including flow controls, and appropriate instrumentation. Figure 6 shows a schematic of the facility and a photograph of the test installation. The rotational speed of the turbine was measured with an electronic counter in conjunction with a magnetic pickup and a shaft-mounted gear. Mass flow was measured with a calibrated venturi. Turbine torque was determined by measuring the reaction torque of the airbrake, which was mounted on air trunnion bearings, and adding corrections for the turbine bearings and seal losses and the coupling windage loss. These tare losses corresponded to about 7.5 percent of the measured torque obtained at design equivalent speed and work factor. The torque load was measured with a commercial strain-gage load cell.

The turbine instrumentation stations are shown in figure 1. Figure 7 shows the instrumentation at each station. Stations 4.5, 5, and 6 were chosen because they corresponded to the station locations in the UGT test engine. Stations 5.5 and 6.3 were added for component testing. Instrumentation at the manifold inlet (station 4.5) measured wall static pressure, total pressure, and total temperature. At both the stator inlet (station 5) and the stator exit (station 5.5) static pressures were measured with six taps, with three each on the inner and outer walls. The inner and outer wall taps were located opposite each other at different intervals around the circumference.

There were two measuring stations at the rotor exit, stations 6 and 6.3. At station 6, located about half an axial chord length downstream of the rotor, static pressures were measured with six taps, with three each on the inner and outer walls. At station 6.3, located about three axial chord lengths downstream of the rotor, static pressure, total pressure, total temperature, and flow
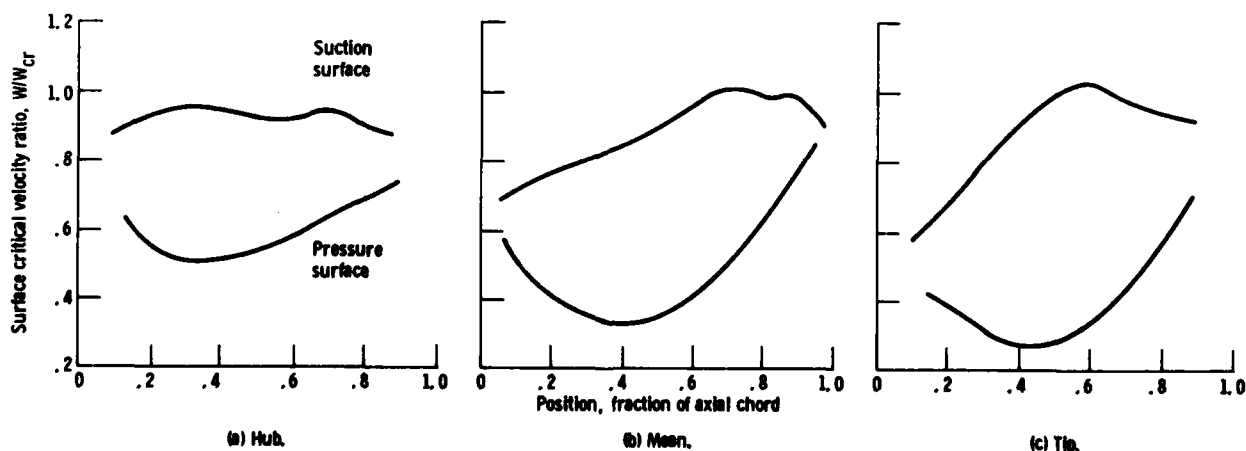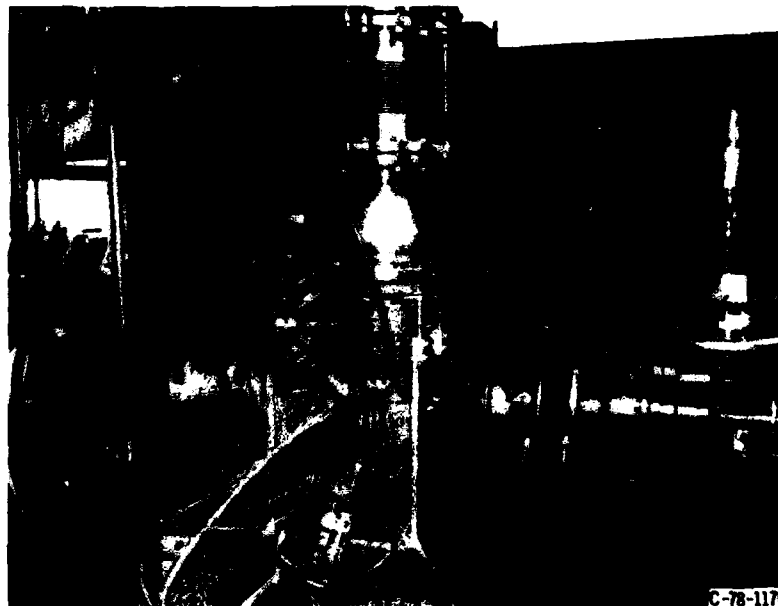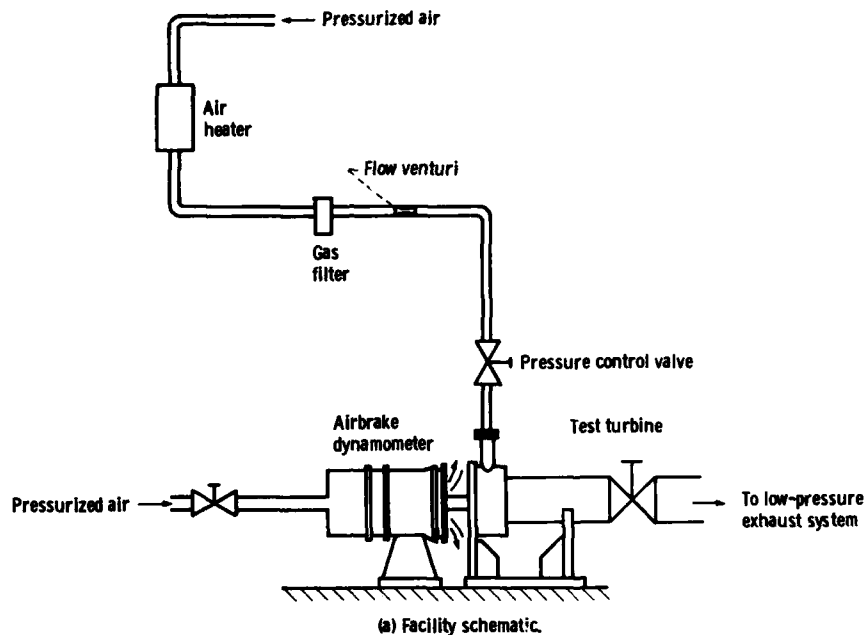

Figure 5. - Rotor blade surface velocity distributions.

(a) Hub.　　(b) Mean.　　(c) Tip.

(a) Facility schematic.

C-78-1170

(b) Turbine test apparatus.

Figure 6. – Test installation.

angle were measured. The static pressure was measured with six taps, with three each on the inner and outer walls. Three self-aligning probes located around the circumference were used for measurement of total pressure, total temperature, and flow angle. The location of station 6.3 was determined by using a hot-wire anemometer survey probe at several axial locations downstream of the rotor so that rotor-exit instrumentation could be located where there would be no rotor wake effects.

The stage test program consisted of three parts: Part one determined the turbine performance with the as-cast blading over a range of equivalent total pressure ratios and rotative speeds. The manifold-inlet-total-to-rotor-exit-total pressure ratio was varied from 1.3 to 2.7 and the speed from 50 to 110 percent of equivalent design
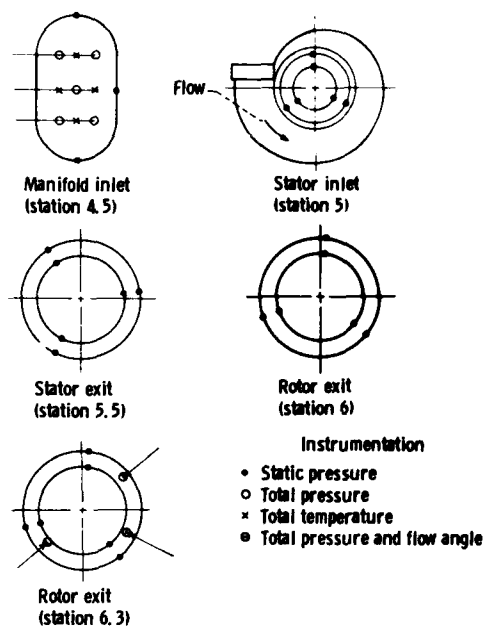
7

Manifold inlet
(station 4.5)

Stator inlet
(station 5)

Flow

Stator exit
(station 5.5)

Rotor exit
(station 6)

Instrumentation
- • Static pressure
- ○ Total pressure
- × Total temperature
- ⊖ Total pressure and flow angle

Rotor exit
(station 6.3)

Figure 7. – Flow path instrumentation, viewed looking downstream.

speed. The tests were conducted at the hot-engine Reynolds number that is listed in table I. Part two determined the turbine performance of the reduced-blade-surface-roughness and the reworked-rotor-profile configurations. These two modified rotor configurations were evaluated over a range of turbine pressure ratios at equivalent design speed. Part three was a Reynolds number evaluation of all three rotor configurations. Reynolds number was changed from 1.2×10^5 to 8.0×10^5 over a range of turbine pressure ratio at design equivalent speed. Reynolds number was changed by varying the turbine-inlet total pressure.

In each part of the test program a rotor-exit radial survey was first conducted at equivalent design values of speed and specific work. Mass-averaged values of flow angle, total temperature, and total pressure were

obtained for each of the three circumferential survey locations at station 6.3. These mass-averaged values were then arithmetically averaged to obtain overall values. The survey probes were then positioned with one each near the tip, near midspan, and near the hub so that the average flow angle from these three positions would correspond closely to the overall mass-averaged value obtained from the survey. Performance data were then obtained at other operating conditions.

The stage evaluation was conducted in air at nominal inlet conditions of 320 K and a range of turbine-inlet pressures from 0.4 to 2.4 bars absolute. The turbine was rated on the basis of total efficiency. The actual work was calculated from torque, speed, and mass flow measurements. The ideal work was based on the manifold-inlet-to-rotor-exit total pressure ratio. The manifold-inlet (station 4.5) and rotor-exit (station 6.3) total pressures were calculated from mass flow, static pressure, total temperature, and flow angle. For the calculation of manifold-inlet total pressure the flow angle was assumed to be zero.

Results and Discussion

The turbine performance results from this experimental investigation are presented in four sections: The first section presents the measured performance of the as-cast blading. Mass flow and torque data as well as a turbine map and the results of a rotor-exit survey are presented. The second section presents the turbine performance changes, at 100 percent of design speed, as the rotor blade profiles were, first, polished to reduce the surface roughness and, second, reworked to more nearly match the design profile. The third section presents the effect of Reynolds number on stage performance for each of the rotor configurations. In the last section a comparison is made between the reworked UGT compressor-drive turbine and the compressor-drive turbine of the baseline gas turbine engine.
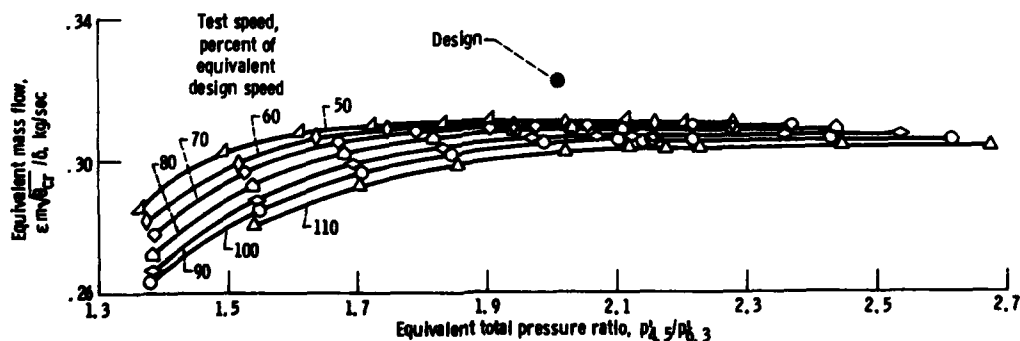

Figure 8. – Variation of equivalent mass flow with total pressure ratio and speed; as-cast blading.

8

Performance of As-Cast Blading

Mass flow. – The variation in equivalent mass flow with equivalent total pressure ratio and rotor speed is shown in figure 8. The equivalent design mass flow given in the figure is the design mass flow value for cold hardware that is listed in table 1. The data in figure 8 show that at the two lowest rotor speeds tested the stator choked before the rotor but as the rotor speed was increased the rotor choked first. At 100 percent of equivalent design speed and at the equivalent design total pressure ratio of 2.01, the measured mass flow was 0.306 kg/sec, which is 6 percent less than the design flow. Both the stator and rotor throat areas were measured and, when compared with the cold design areas, were found to be 4.1 and 6.3 percent smaller, respectively. This mismatch in stator and rotor flow areas caused a redistribution of pressure in the turbine, which in turn changed the flow characteristic of the machine. It appears, however, that most of the mass flow deficit was caused by the undersized hardware.

Torque. – The variation of equivalent torque with equivalent total pressure ratio for the equivalent speeds tested is shown in figure 9. The design value of torque shown in the figure is the design value for a cold turbine. At the equivalent design conditions of 100 percent speed and a total pressure ratio of 2.01 the measured torque was 4.36 N-m. This is 12.6 percent lower than the design torque. Six percent of this deficit was due to the shortfall in mass flow of the turbine, and the remaining 6.6 percent was caused by increased aerodynamic losses.

Performance map. – The performance map shown in figure 10 was generated from the mass flow and torque
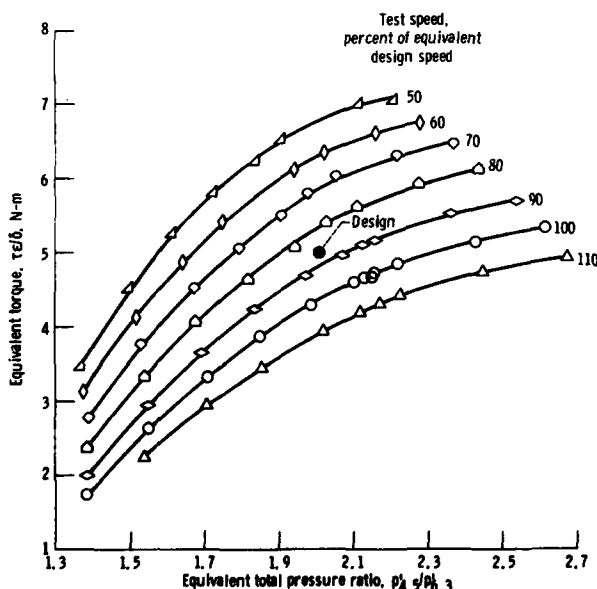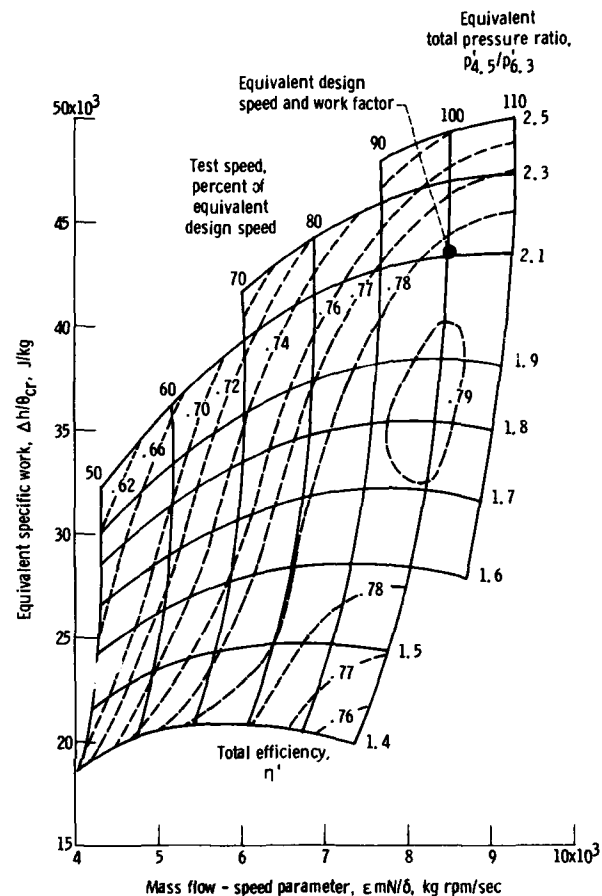

Figure 10. – Compressor-drive turbine performance map; as-cast blading.

data of figures 8 and 9. At a given pressure ratio, and for each speed, smooth-curve values of torque and mass flow were used to calculate the equivalent specific work $\Delta h/\theta_{cr}$, the mass flow-speed parameter $\epsilon mN/\delta$, and the total efficiency η'.

The turbine attained efficiencies of 0.62 to 0.79 over the range of test conditions. At the equivalent design speed and work factor the turbine efficiency was 0.783, which is 0.067 less than the design efficiency of 0.85. A significant part of this deficit was caused by manufacturing imperfections in the rotor blade profiles, as is discussed later in this report.

Rotor-exit survey. – The results of the radial surveys at station 6.3 of flow angle, total pressure, and total temperature are shown in figures 11(a), (b), and (c). The measurements were taken with the turbine operating at equivalent design speed and specific work. The data shown are the averages of the measurements of the three combination probes. With these measurements the radial variation in stage efficiency was calculated and is presented in figure 11(d). The dashed curves in the figures
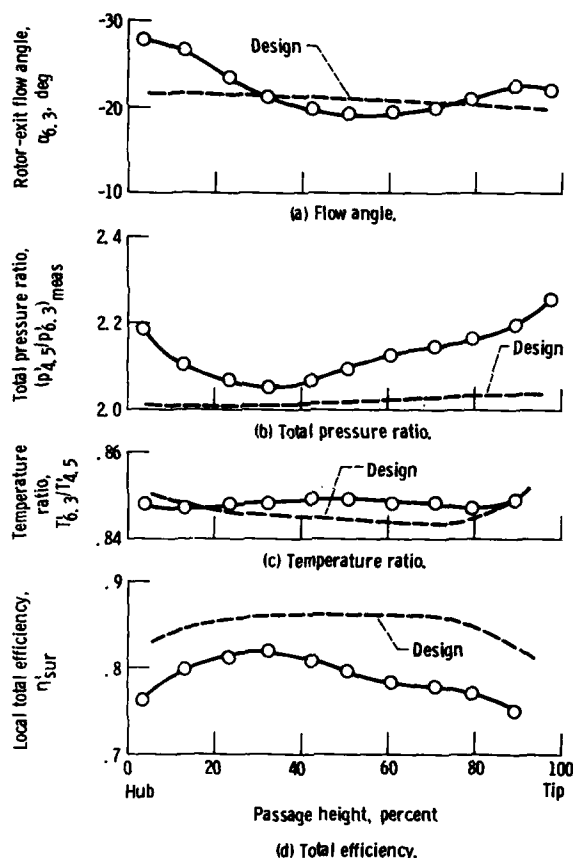

Figure 9. - Variation of torque with total pressure ratio and speed; as-cast blading.

9

(a) Flow angle.

(b) Total pressure ratio.

(c) Temperature ratio.

(d) Total efficiency.

Figure 11. – Turbine-exit survey at equivalent design speed and specific work; as-cast blading.

represent the calculated design radial variations at the turbine exit.

The flow angle measured was within $\pm 2°$ of the design variation over most of the blade sp.. except near the hub. At the hub the flow was overturned. This overturning may have been caused by secondary flows at the hub.

The stage pressure ratio (fig. 11(b)) was significantly higher than the design variation over most of the passage height. It is believed that the thickened blade profiles increased the rotor trailing-edge mixing losses, resulting in a higher than design pressure ratio across the entire passage height. In addition, thick turbine-inlet boundary layers and stator incidence near the endwalls most likely caused higher pressure ratios in those regions. The manifold-stator tests (ref. 6) indicated a turbine-inlet hub boundary layer equal to 20 percent of the passage height and positive stator incidence up to 20°. At the tip the inlet boundary layer and stator incidence, although reduced, were still significant.

The temperature measurements (fig. 11(c)) indicated nearly constant work extraction radially and agreed well with the design variation. The radial variation in stage

efficiency (fig. 11(d)) reached a maximum value of 0.82 at about 30 percent of passage height and then fell off toward both endwalls. The probable reasons for the decrease in efficiency are the same as those that caused the increase in stage pressure ratio. The rotor-exit survey results were also used to calculate a mass-averaged turbine efficiency. The value calculated was 0.781, which is in excellent agreement with the value of 0.783 obtained from torque, speed, and mass flow.

Effect of Rotor Blade Profile Imperfections

As mentioned earlier the turbine blade rows used for component testing were duplicates of the stator and rotor castings used in the engine. Inspection of the rotor blading before the start of the turbine testing showed significant deviations from design in the profile shape and a fairly rough surface. Figure 12 compares inspection tracings of the mean and tip sections with the design profile of two randomly selected rotor blades. Hub section tracings were not obtained because the tracing stylus was too large to fit in the small hub area.

Because of the condition of the as-received rotor casting, two modifications were made to the rotor blading after completing the performance tests of the as-
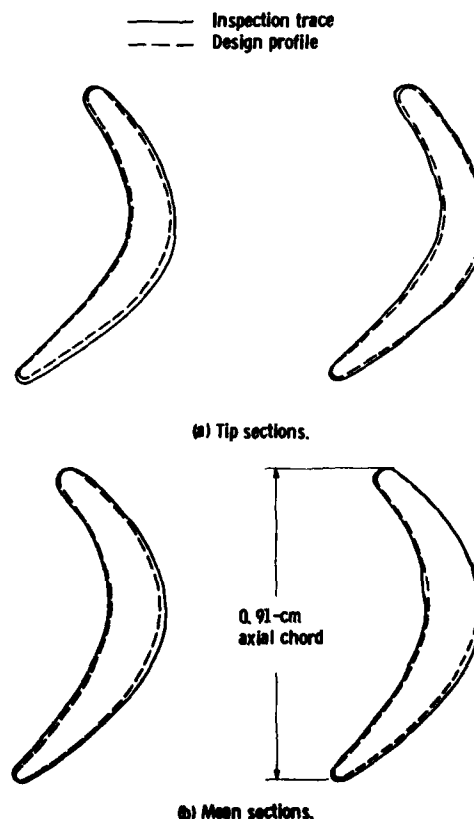

——— Inspection trace
— — — Design profile

(a) Tip sections.

0.91-cm axial chord

(b) Mean sections.

Figure 12. – Comparison of design and as-cast rotor blade profiles.

10

cast blading. The first modification consisted of reducing the blade surface roughness by polishing the suction surface of each blade and applying a thin coat of lacquer to the pressure surfaces. Tests were then made with this configuration. The second modification consisted of electric discharge machining the rotor profiles to the design profile. Inspection traces at the mean and tip of the machined rotor agreed closely with the design profile, but rotor throat measurements indicated that the hub section was still thick. However, any further hub machining may have resulted in undersized profiles away from the hub, so no additional machining was attempted. The respective suction- and pressure-surface roughness measurements of the reworked rotor were essentially the same as those measured after polishing and coating the as-cast rotor. Tests were then conducted on the reworked rotor blading. Table IV lists selected geometric measurements of the three rotors. Reference 7 gives additional details of the blading modifications and test results. The chief findings of the effect of these rotor blading changes on the turbine performance are summarized in the following paragraphs.

Mass flow and overall efficiency. – The variations in equivalent mass flow and efficiency with the stage total pressure ratio at equivalent design speed are shown in figure 13. The lowest mass flow was measured with the as-cast rotor and the highest mass flow with the reworked rotor, but the difference was small, only about 0.7 percent at the pressure ratio of 2.01. The flow area increase of the reworked rotor was 3 percent. These results indicate that at this rotor speed the as-cast rotor choked just before the stator but that with the reworked rotor installed the stator choked first and therefore limited the stage mass flow. The difference in efficiency between the as-cast and reduced-roughness rotors was nominally 1 point and that between the as-cast and reworked-profile rotors was nominally 4 points. At the design value of specific work the turbine efficiencies were
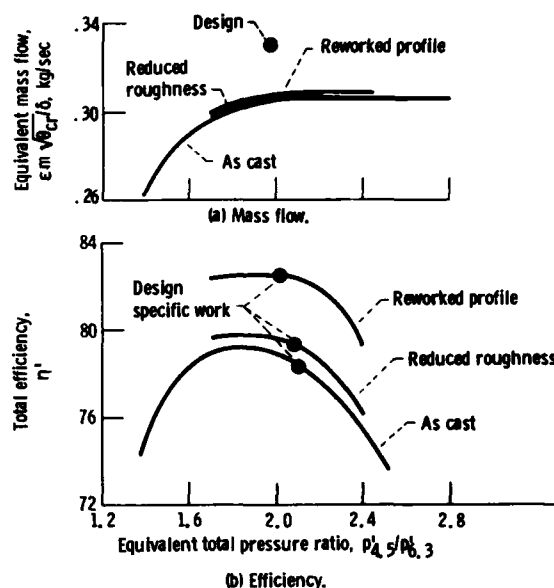

(a) Mass flow.

(b) Efficiency.

Figure 13. - Variation of mass flow and efficiency with pressure ratio at design speed for three rotor configurations.

0.783, 0.794, and 0.825 for the as-cast, reduced-roughness, and reworked-profile configurations, respectively. According to influence coefficients for the UGT engine cycle, an increase of 4 points in compressor turbine efficiency would have increased the engine power 7.5 percent.

Radial variation in efficiency. – The radial variations in turbine efficiency calculated from rotor-exit measurements of total temperature, total pressure, and flow angle are shown in figure 14. As can be seen the largest increase in efficiency obtained by improving the surface finish and reducing the blade thickness occurred from midspan out to the tip. This may have occurred because, as mentioned earlier, it was difficult to improve

TABLE IV. - ROTOR GEOMETRIC COMPARISON

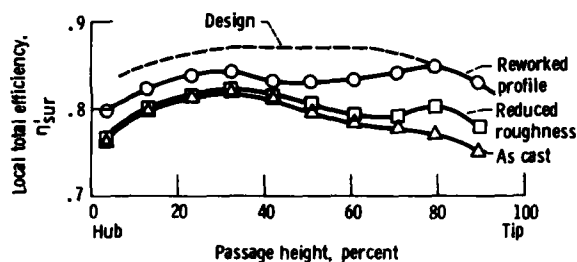| Parameter	Design	As cast	Reduced roughness	Reworked profile
Surface finish, μm:				
Suction surface	(a)	1.35	0.33	0.33
Pressure surface	(a)	1.35	0.95	0.95
Average trailing-edge thickness, cm	0.038	0.053	0.053	0.042
Average trailing-edge blockage, percent	11.8	16.5	16.5	13.0
Profile tolerance, mm	±0.1	±0.15 max	±0.15 max	±0.025

ᵃSpecification unknown.

Figure 14. – Radial variation in efficiency at design speed and specific work for three rotor configurations.

the blade profile near the hub. Also to be noted is that the radial variation in efficiency for the reworked rotor approached the same shape as the design variation although the level was lower. Mass-averaged efficiencies were calculated from these data and compared with the corresponding efficiencies shown in figure 13. The maximum difference between the two methods of calculating the turbine efficiency was 0.8 point.

Causes of performance changes. – The 1-point improvement in stage efficiency resulting from smoothing the rotor blade surfaces was attributed to a lower profile friction loss. A number of possible causes were considered for the additional 3-point gain with the reworked rotor. Possible causes considered in reference 7 were stator and rotor reaction changes, rotor incidence changes, and differences in the rotor trailing-edge losses. Test data were used to calculate stage velocity diagrams for all three rotor configurations. On the basis of those calculations it was concluded that the reaction and incidence changes were not large enough to be a major factor contributing to the change in performance. An analysis of rotor trailing-edge losses, however, did indicate that most of the performance gain between the as-cast thick and thinned rotor blades, both with the same surface finish, was due to reduced trailing-edge losses of the reworked blades.

Effect of Reynolds Number

Reynolds number tests were made for all three rotor configurations. As mentioned earlier the Reynolds number was varied by varying the turbine-inlet pressure. For each pressure the Reynolds number and the turbine efficiency were calculated, from smooth-curve data, at the design work factor of 2.1. The results are shown in figure 15. The turbine design Reynolds number at hot-engine conditions was 2.44×10^5.

The turbine efficiency with the as-cast and reduced-roughness blading showed steady improvement with Reynolds number over most of the range of Reynolds number tested. The as-cast blading efficiency leveled out at a value of 0.796 when the Reynolds number was 6.0×10^5 or higher. The effect of Reynolds number on the performance of the reworked rotor was very slight. No

increase in efficiency was measured for Reynolds numbers above the turbine design value, and only a slight decrease was noted at lower values.

Several equations have been used in attempts to correlate turbine efficiency with Reynolds number. A frequently used form from reference 10 is

$$\frac{1-\eta_1'}{1-\eta_2'} = A + B\left(\frac{Re_2}{Re_1}\right)^{0.2} \tag{1}$$

where $A + B = 1$. The coefficients A and B are used to proportion the turbine losses between viscous and nonviscous effects. The subscripts 1 and 2 correspond to separate points on a performance curve of efficiency versus Reynolds number. The reference suggests that A ranges from 0.3 to 0.4 and the corresponding range for B is 0.7 to 0.6. This equation, with $A = 0.4$ and $B = 0.6$, overestimates the effect of Reynolds number for all the rotor configurations for the range of Reynolds number investigated. It may, however, provide a reasonable correlation at lower Reynolds numbers. The preceding equation appears to oversimplify the correlation of loss with Reynolds number. Additional but at this time unknown factors, perhaps both aerodynamic and geometric, are needed to provide a better correlation of turbine loss with Reynolds number.

Comparison of Upgraded and Baseline Compressor-Drive Turbines

The performance of the reworked upgraded compressor-drive turbine was compared with that of the baseline compressor-drive turbine to determine if a performance gain was realized. The performance of the baseline turbine is reported in reference 11. Most experimental procedures used to evaluate the two turbines were identical except for the method used to calculate the turbine pressure ratio, which in turn was used to calculate the efficiency.

The baseline turbine pressure ratio was determined from measurements of total pressure at the manifold inlet (station 4.5) and at the mean radius 1/2 blade chord downstream of the rotor (a location corresponding to
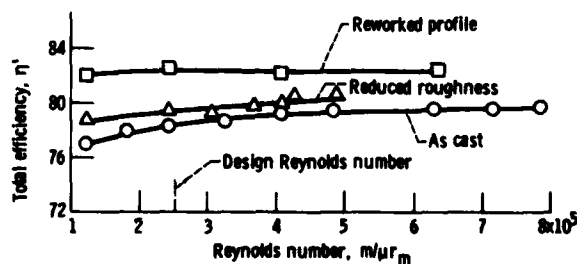

Figure 15. – Variation of turbine performance with Reynolds number for three rotor configurations.

station 6 in fig. 1). This measured pressure ratio was then adjusted to agree with the mass-averaged pressure ratio obtained from radial surveys of the flow at station 6. Station 6 was used for the baseline turbine because there was a diffusing interstage duct downstream of that station.

As mentioned earlier the upgraded turbine was tested with a constant-area exhaust duct, and hot-wire measurements were taken to find an axial location (station 6.3, fig. 1) where no rotor wakes were distinguishable. Radial surveys of the upgraded turbine were taken at stations 6 and 6.3, and the turbine efficiency was calculated from mass-averaged as well as calculated total pressures at the two stations. The calculated total pressure was obtained from continuity and energy considerations as described in the section **Research Equipment and Procedure.** The upgraded turbine efficiency based on the mass-averaged pressure at station 6.3 and the efficiencies based on the calculated total pressures at stations 6 and 6.3 were nearly identical and were nominally 2 points lower than the efficiency calculated from the mass-averaged pressure at station 6. This difference in efficiency was attributed to the loss caused by rotor wake mixing, which was not complete at station 6. Therefore, it was concluded that the efficiencies reported for the baseline turbine (ref. 11) did not include the total rotor wake mixing loss. Because of that the baseline turbine efficiency was recalculated by using a calculated total pressure at station 6. It is that baseline turbine efficiency that is compared with the upgraded turbine efficiency.

Selected aerodynamic parameters of the baseline turbine and the upgraded turbine with the reworked profiles are given in table V. The turbine efficiencies listed are the efficiencies with the turbines operating at their respective equivalent design speed and design work factor. As can be noted, the upgraded turbine is smaller than the baseline turbine, has less rotor reaction, and has

TABLE V. - COMPARISON OF UPGRADED AND BASELINE

COMPRESSOR-DRIVE TURBINES

Parameter	Baseline	Upgraded
Mass flow rate[a], kg/sec	0.558	0.308
Tip diameter, cm	14.0	11.1
Tip clearance, percent	1.7	1.7
Rotor trailing-edge blockage, percent	10.8	13
Design work factor	2.4	2.1
Design Reynolds number, $m/\mu r_m$	3.3×10^5	2.44×10^5
Rotor mean reaction[a], $R_{x,m}$	0.31	0.20
Measured stage efficiency[a], η'	0.803	0.825

[a]From measurements taken at design work factor, Reynolds number, and speed.

a slightly lower aerodynamic loading as indicated by the work factor. The smaller size of the upgraded turbine resulted in more rotor trailing-edge blockage and a lower Reynolds number. These aerodynamic features of the upgraded turbine, with the exception of the lower work factor, increased the difficulty of obtaining high turbine efficiency. However, the upgraded turbine achieved a 2-point improvement over the baseline turbine. This improvement is probably due to the use of improved design computer codes between the time the baseline turbine was designed and the time the upgraded turbine was designed.

Concluding Remarks

The results of this program are encouraging and indicate that attaining the efficiency goal of 0.85 for an axial turbine the size of the upgraded turbine is not unrealistic. A number of design and hardware deficiencies have been identified, and correction of these would improve the turbine performance. The corrections include reducing the inlet boundary layers and stator incidence, fabricating more accurately the stator and rotor profiles, and improving the profile surface finish. Fewer, longer chord blades would reduce the rotor trailing-edge loss, which was found to have a significant effect on performance. Because this change would also reduce the blade aspect ratio, a balance between the two effects is necessary. Finally, the application of stator endwall contouring and nonuniform radial work distribution may also be beneficial.

Summary of Results

The aerodynamic performance of the compressor-drive turbine of the Department of Energy Upgraded Gas Turbine engine was determined in air at nominal inlet conditions of 320 K and 0.8 bar absolute. Three modifications of the same rotor design were tested: an as-cast rotor, the same rotor with reduced surface roughness, and the rotor with thinned blade profiles. Reynolds number tests were made with all three rotors by varying the inlet pressure between 0.4 and 2.4 bars absolute. The results of the investigation were as follows:

1. The turbine efficiency at design speed and work factor with the as-cast blading was 0.783. The efficiency increased to 0.794 after the blade surface roughness was reduced and reached 0.825 after the rotor profiles were thinned.

2. The performance of the turbine with the as-cast blades varied with Reynolds number. The efficiency of the as-cast turbine leveled out at a maximum value of 0.796 at a Reynolds number of 6.0×10^5. There was very little effect of Reynolds number with the rotor blades thinned and smoothed.

3. The change in efficiency with Reynolds number for all turbine configurations tested was not satisfactorily predicted by the equation

$$\frac{1-\eta_1'}{1-\eta_2'} = A + B\left(\frac{Re_2}{Re_1}\right)^{0.2}$$

where η' is the efficiency based on total pressure ratio, the subscripts 1 and 2 correspond to separate points on a performance curve of efficiency versus Reynolds number, Re is Reynolds number, and the coefficients A and B are used to proportion the turbine losses between viscous and nonviscous effects.

4. At their respective design conditions the upgraded turbine achieved a 2-point improvement in efficiency over the baseline turbine.

References

1. Ball, G. A.; Gumaer, J. I.; and Sebestyen, T. M.: The ERDA/Chrysler Upgraded Gas Turbine Engine Objectives and Design. SAE Paper 760279, 1976.
2. Galvas, M. R.: A Compressor Designed for the Energy Research and Development Agency Automotive Gas Turbine Program. NASA TM X-71719, 1975.
3. Roelke, R. J.; and McLallin, K. L.: The Aerodynamic Design of a Compressor-Drive Turbine for Use in a 75 kW Automotive Engine. NASA TM X-71717, 1975.
4. Kofskey, M. G.; Katsanis, T.; and Schumann, L. F.: Aerodynamic Design of a Free Power Turbine for a 75 kW Gas Turbine Automotive Engine. NASA TM X-71714, 1975.
5. McLallin, K. L.; Kofskey, M. G.; and Wong, R. Y.: Cold-Air Performance of a 15.41-cm-Tip-Diameter Axial-Flow Power Turbine with Variable-Area Stator Designed for a 75-kW Automotive Gas Turbine Engine. NASA TM-82644, DOE/NASA/51040-30, 1982.
6. Roelke, R. J.; and Haas, J. E.: Cold-Air Performance of Compressor-Drive Turbine of Department of Energy Upgraded Automobile Gas Turbine Engine. I – Volute-Manifold and Stator Performance. NASA TM-82682, 1981.
7. Roelke, R. J.; and Haas, J. E.: The Effect of Rotor Blade Thickness and Surface Finish on the Performance of a Small Axial Flow Turbine. ASME Paper 82-GT-222, 1982.
8. Wagner, C. E.; and Pampreen, R. C.: Upgraded Automotive Gas Turbine Engine Design and Development Program Final Report. (COO-2749-43-VOL-2, Chrysler Corp.; EY-76-C-02-2749.) NASA CR-159671, DOE/NASA/2749-79/2-VOL-2, 1979.
9. Katsanis, T.: FORTRAN Program for Calculating Transonic Velocities on a Blade-to-Blade Stream Surface of a Turbomachine. NASA TN-5427, 1969.
10. Glassman, A. J.: Turbine Design and Application. NASA SP-290, Vol. 1, 1972, p. 60.
11. Roelke, R. J.; and McLallin, K. L.: Cold-Air Performance of the Compressor-Drive Turbine of the Department of Energy Baseline Automobile Gas-Turbine Engine. NASA TM-78894, 1978.

14

1. Report No. NASA TM-82818 AVRADCOM TR 82-C-1	2. Government Accession No. AD-A121 041	3. Recipient's Catalog No.
4. Title and Subtitle COLD-AIR PERFORMANCE OF COMPRESSOR-DRIVE TURBINE OF DEPARTMENT OF ENERGY UPGRADED AUTOMOBILE GAS TURBINE ENGINE II - STAGE PERFORMANCE		5. Report Date OCTOBER 1982
		6. Performing Organization Code 505-32-2B
7. Author(s) Richard J. Roelke and Jeffrey E. Haas		8. Performing Organization Report No. E-1165
		10. Work Unit No.
9. Performing Organization Name and Address NASA Lewis Research Center and AVRADCOM Research and Technology Laboratories Cleveland, Ohio 44135		11. Contract or Grant No.
		13. Type of Report and Period Covered Technical Memorandum
12. Sponsoring Agency Name and Address U.S. Department of Energy Office of Vehicle and Engine R&D Washington, D.C. 20545		14. Sponsoring Agency Code Report No. DOE/NASA/1011-36

16. Abstract
The aerodynamic performance of the compressor-drive turbine of the DOE Upgraded Gas Turbine engine was determined in low-temperature air. The as-received cast rotor blading had a significantly thicker profile than design and a fairly rough surface finish. Because of these blading imperfections a series of stage tests with modified rotors were made. These included the as-cast rotor, a reduced-roughness rotor, and a rotor with blades thinned to near design. Significant performance changes were measured. Tests were also made to determine the effect of Reynolds number on the turbine performance. Comparisons are made between this turbine and the compressor-drive turbine of the DOE baseline gas turbine engine.

17. Key Words (Suggested by Author(s)) Automotive gas turbine engine; Small axial flow turbine performance; Effect of blade profile inaccuracies; Reynolds number	18. Distribution Statement Unclassified - unlimited STAR Category 02 DOE Category UC-96

19. Security Classif. (of this report) Unclassified	20. Security Classif. (of this page) Unclassified	21. No. of Pages 16	22. Price* A02

* For sale by the National Technical Information Service, Springfield, Virginia 22161

NASA-Langley, 1982

ATE
MED